

## **SUPPORTING INFORMATION (SI)**

### **Thermodynamics and crystal chemistry of rhomboclase, (H<sub>5</sub>O<sub>2</sub>)Fe(SO<sub>4</sub>)<sub>2</sub>·2H<sub>2</sub>O, and the phase (H<sub>3</sub>O)Fe(SO<sub>4</sub>)<sub>2</sub>**

JURAJ MAJZLAN<sup>1,\*</sup>, KLAUS-DIETER GREVEL<sup>1</sup>, BORIS KIEFER<sup>2</sup>, ULLA GRO NIELSEN<sup>3</sup>, ELISABETH GRUBE<sup>3,4</sup>,  
EDGAR DACHS<sup>5</sup>, ARTUR BENISEK<sup>5</sup>, MARY ANNE WHITE<sup>6</sup>, MICHEL B JOHNSON<sup>6</sup>

<sup>1</sup>Institute of Geosciences, Friedrich-Schiller-University, Carl-Zeiss Promenade 10, D-07745 Jena, Germany

<sup>2</sup>Department of Physics, 153 Gardiner Hall, New Mexico State University, Las Cruces 88003, New Mexico, USA

<sup>3</sup>Department of Physics, Chemistry, and Pharmacy, University of Southern Denmark, Campusvej 55, 5230 Odense M, Denmark

<sup>4</sup>Current address: Interdisciplinary Nanoscience Center and Department of Chemistry, Aarhus University, Langelandsgade 140, 8000, Århus C, Denmark

<sup>5</sup>Department of Chemistry and Physics of Materials, Division Mineralogy, University of Salzburg, Hellbrunnerstrasse 34, A-5020 Salzburg, Austria

<sup>6</sup>Department of Chemistry and Institute for Research in Materials, Dalhousie University, Halifax, NS B3H 4R2, Canada

\*Corresponding author:

Institute of Geosciences

Friedrich-Schiller-University

Carl-Zeiss Promenade 10

D-07745 Jena, Germany

Telephone: +49-3641-948700

Fax: +49-3641-948602

e-mail: Juraj.Majzlan@uni-jena.de

Number of figures: 1

Number of tables: 3

Total number of pages in SI: 7

Table S1. Initial composition of the charges used to determine solubility of ferric sulfate phases at room temperature. These charges were maintained at room temperature (22±3 °C) for 3 years. Sulfuric acid is 98 % H<sub>2</sub>SO<sub>4</sub>, ferric sulfate is X-ray amorphous powder with approximate composition Fe<sub>2</sub>(SO<sub>4</sub>)<sub>3</sub>·6.75H<sub>2</sub>O.

| sample | water<br>(mL) | sulfuric<br>acid<br>(mL) | ferric<br>sulfate<br>(g) | sample<br>(mL) | water<br>acid<br>(mL) | sulfuric<br>sulfate<br>(g) | ferric |
|--------|---------------|--------------------------|--------------------------|----------------|-----------------------|----------------------------|--------|
| TB-1   | 2.6729        | 0.060                    | 4.2278                   | TB-12          | 3.3525                | 0.870                      | 2.0520 |
| TB-2   | 2.7766        | 0.200                    | 3.8712                   | TB-13          | 3.3998                | 0.910                      | 1.9338 |
| TB-2-1 | 2.7860        | 0.208                    | 3.8384                   | TB-14          | 3.4159                | 0.935                      | 1.8740 |
| TB-2-2 | 2.7973        | 0.217                    | 3.8122                   | TB-15          | 3.4313                | 0.951                      | 1.8180 |
| TB-2-3 | 2.8056        | 0.226                    | 3.7731                   | TB-16          | 3.4404                | 0.980                      | 1.7487 |
| TB-2-4 | 2.8170        | 0.236                    | 3.7523                   | TB-17          | 3.4592                | 1.000                      | 1.7010 |
| TB-2-5 | 2.8281        | 0.245                    | 3.7206                   | TB-18          | 3.4375                | 1.010                      | 1.6986 |
| TB-2-6 | 2.8361        | 0.253                    | 3.6931                   | TB-19          | 3.4522                | 1.030                      | 1.6350 |
| TB-2-7 | 2.8456        | 0.265                    | 3.6587                   | TB-20          | 3.4801                | 1.082                      | 1.5255 |
| TB-2-8 | 2.8566        | 0.272                    | 3.6322                   | TB-21          | 3.4640                | 1.092                      | 1.5221 |
| TB-2-9 | 2.8660        | 0.281                    | 3.6030                   | TB-22          | 3.5059                | 1.140                      | 1.4069 |
| TB-3   | 2.8746        | 0.290                    | 3.5708                   | TB-23          | 3.5444                | 1.150                      | 1.3494 |
| TB-4   | 3.0183        | 0.417                    | 3.2198                   | TB-24          | 3.5705                | 1.195                      | 1.2314 |
| TB-5   | 3.1061        | 0.520                    | 2.9937                   | TB-25          | 3.5996                | 1.243                      | 1.1079 |
| TB-6   | 3.1587        | 0.620                    | 2.6964                   | TB-26          | 3.6262                | 1.299                      | 0.9934 |
| TB-7   | 3.1931        | 0.678                    | 2.5221                   | TB-27          | 3.6269                | 1.423                      | 0.7611 |
| TB-8   | 3.2946        | 0.711                    | 2.4016                   | TB-28          | 3.6587                | 1.508                      | 0.5893 |
| TB-9   | 3.3161        | 0.760                    | 2.2894                   | TB-29          | 3.6143                | 1.660                      | 0.3470 |
| TB-10  | 3.3307        | 0.790                    | 2.2273                   | TB-30          | 3.5242                | 1.798                      | 0.1732 |
| TB-11  | 3.3393        | 0.843                    | 2.1086                   |                |                       |                            |        |

Table S2. Initial composition of the charges used to determine solubility of ferric sulfate phases at near-freezing temperature. These charges were maintained at 4 °C for 5 years. Sulfuric acid is 98 % H<sub>2</sub>SO<sub>4</sub>, ferric sulfate is X-ray amorphous powder with approximate composition Fe<sub>2</sub>(SO<sub>4</sub>)<sub>3</sub>·6.75H<sub>2</sub>O.

| sample | water<br>(mL) | sulfuric<br>acid<br>(mL) | ferric<br>sulfate<br>(g) |
|--------|---------------|--------------------------|--------------------------|
| TB1-K  | 2.6745        | 0.055                    | 4.2182                   |
| TB3-K  | 2.8795        | 0.305                    | 3.5739                   |
| TB5-K  | 3.1017        | 0.525                    | 2.9326                   |
| TB7-K  | 3.2239        | 0.680                    | 2.5224                   |
| TB9-K  | 3.3184        | 0.765                    | 2.2872                   |
| TB11-K | 3.3327        | 0.840                    | 2.1074                   |
| TB13-K | 3.4036        | 0.909                    | 1.9267                   |
| TB15-K | 3.4286        | 0.950                    | 1.8195                   |
| TB17-K | 3.4557        | 0.999                    | 1.6995                   |
| TB19-K | 3.4562        | 1.039                    | 1.6353                   |
| TB21-K | 3.4664        | 1.095                    | 1.4232                   |
| TB23-K | 3.5433        | 1.149                    | 1.3519                   |
| TB25-K | 3.6016        | 1.250                    | 1.1118                   |
| TB27-K | 3.6243        | 1.429                    | 0.7626                   |
| TB29-K | 3.6145        | 1.650                    | 0.3490                   |

### Comparison of the solubility calculation for hydronium jarosite using the Davies equation and the Pitzer model

Figure S1 compares the calculated solubility curves for hydronium jarosite, using the two activity-molality models. It contains the experimental data of Posnjak and Merwin (1922) and solubility of hydronium jarosite calculated by two different approaches. The first one is the application of the Pitzer model of Tosca et al. (2007). The second one is a calculation with the software suite PHREEQC (Parkhurst and Appelo 1999). PHREEQC uses the Davies equation for the calculation of activity coefficients. Admittedly, this equation is not applicable to some of the higher solution molalities plotted in Figure S1 but the goal was a crude test of the performance of the two models, not fine tuning of details. Solubility calculated by full speciation calculations by PHREEQC (using the Davies equation for activity coefficients) fits the experimental data much better than the Pitzer model. Just as for rhomboclase, we observe a distinct shift of the Pitzer-predicted solubility from the experimental data, a shift into the field of the aqueous phase. The Pitzer model predicts the phase diagram qualitatively in terms of its general topology, but the quantitative agreement with the available experimental data remains poor.

One can only speculate about the reasons for these discrepancies. The most likely cause lies in the speciation of Fe(III) and sulfate. The Pitzer model considers  $\text{Fe}^{3+}$ ,  $\text{SO}_4^{2-}$ ,  $\text{HSO}_4^-$ , and  $\text{H}^+$  as the aqueous species. Speciation is calculated iteratively and the interaction parameters were fitted for these species. The calculations with PHREEQC, however, show that  $\text{Fe}^{3+}$  and  $\text{SO}_4^{2-}$  are minor to negligible species at all concentrations except for those at which no Pitzer model is needed. Instead, the entire area shown in Fig. S1 is dominated by  $\text{FeSO}_4^+$  and  $\text{FeHSO}_4^{2+}$  as the Fe(III) species. As for sulfate,  $\text{HSO}_4^-$  predominates essentially everywhere. The consideration of these species in a complicated model (such as the Pitzer model) will modify the actual ionic strength of the solutions for each  $\text{Fe}_2(\text{SO}_4)_3$  and  $\text{H}_2\text{SO}_4$  molality, and hence also the parametrization of the model. The uneasy task of the modification of the Pitzer model should be undertaken in the future, if a model with better performance should eventually be developed.

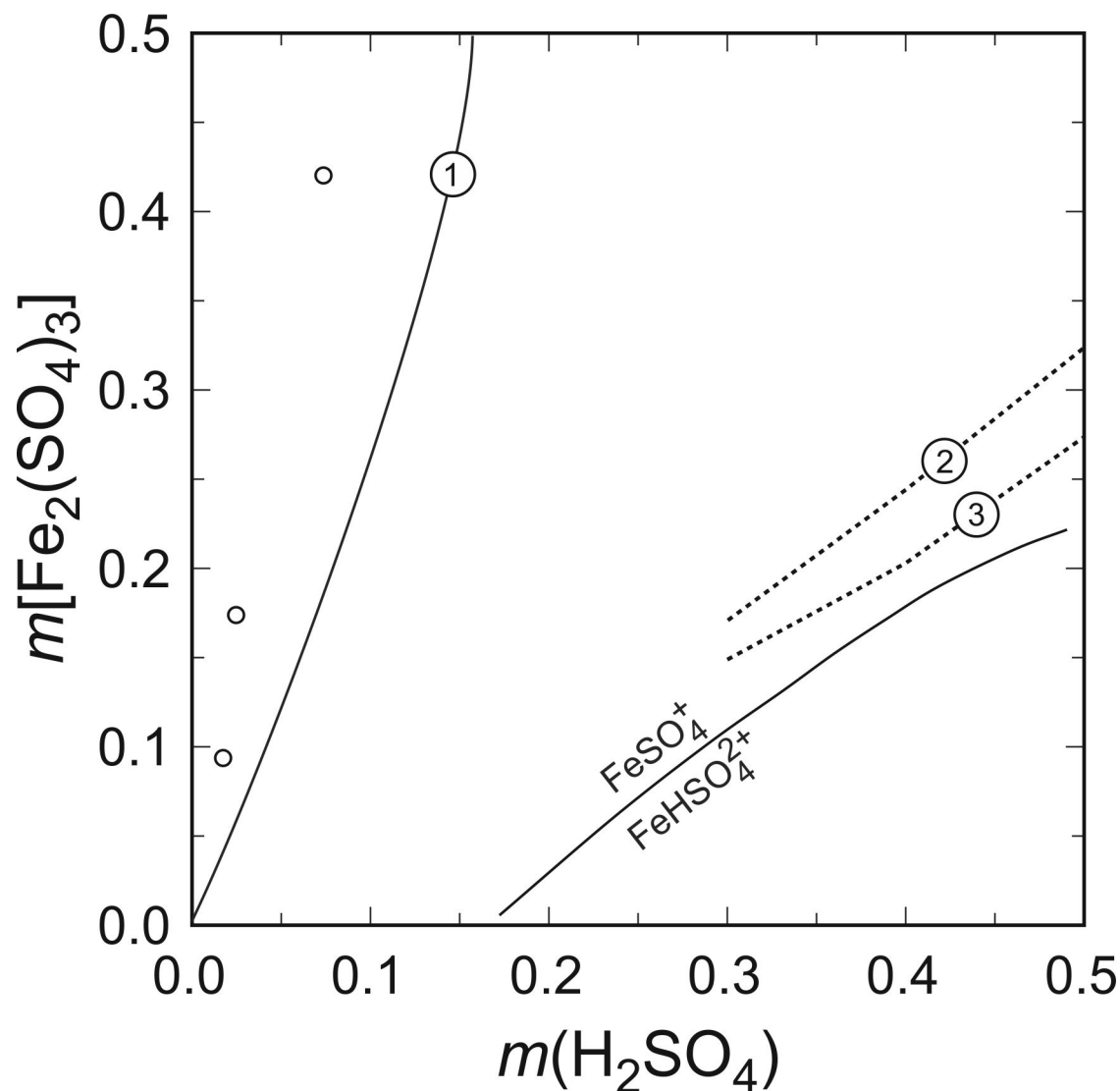


**FIGURE S1.** Experimental (circles, Posnjak and Merwin 1922, 50 °C) and calculated solubilities for hydronium jarosite. Curve 1: calculation by the software PHREEQC (Parkhurst and Appelo 1999), curves 2,3: calculation with the Pitzer model (Tosca et al. 2007) with two different parametrizations of the model. The curve with the two Fe(III) species is the predominance boundary of the two species. The predominance fields of  $\text{Fe}^{3+}$  or other Fe(III) species are too small to be shown in this diagram.

### Measurement and fitting of heat capacity data for rhomboclase

Heat capacity of a rhomboclase sample was measured by relaxation calorimetry. The data are summarized in Table S3. As discussed in the paper, there are severe issues with these data which invalidate them to be used for the calculation of entropy. Despite that, upon the request of the reviewer, we will briefly discuss the data and the fitting procedure. We discourage the use of the data for the derivation of thermodynamic quantities; the location of the magnetic transition at low temperature is probably reliable.

For fitting of the  $C_p$  data below (Table S3), a polynomial  $A_2T^2 + A_4T^4 + A_5T^5$  was found to be the best. The usual Debye polynomial ( $A_3T^3$ ) or extended Debye polynomials ( $A_3T^3 + A_5T^5 + \dots$ ) did not perform well at all. Other polynomials, such as  $A_1T + A_2T^2 + A_3T^3$ , fitted the data well but plunged below zero (i.e., having negative heat capacity) between the data point with the lowest temperature and  $T = 0$  K. The adjustable fit constants were  $A_2 = 0.0642737088683$ ,  $A_4 = 0.02652140004$ , and  $A_5 = -0.00474192604081$ .

For the rest of the data, entropy was calculated by numerical integration, that is, simple addition of trapezoids below the measured data points.

Table S3. Heat capacity data, measured for rhomboclase by relaxation calorimetry in Salzburg (molecular mass 321.03 g·mol<sup>-1</sup>). Temperature (*T*) in K, heat capacity (*C<sub>p</sub>*) in J·K<sup>-1</sup>·mol<sup>-1</sup>.

| <i>T</i> | <i>C<sub>p</sub></i> | <i>T</i> | <i>C<sub>p</sub></i> | <i>T</i> | <i>C<sub>p</sub></i> |
|----------|----------------------|----------|----------------------|----------|----------------------|
| 2.02936  | 0.478404             | 9.35509  | 12.4174              | 43.4844  | 54.1665              |
| 2.20993  | 0.619116             | 9.38423  | 12.6337              | 47.3118  | 61.6923              |
| 2.40796  | 0.794798             | 9.63708  | 15.1374              | 51.4744  | 69.7081              |
| 2.62108  | 1.00412              | 9.88229  | 14.5362              | 56.0194  | 78.0803              |
| 2.85357  | 1.24993              | 10.137   | 11.4927              | 60.9518  | 87.7601              |
| 3.10623  | 1.54468              | 10.1775  | 11.369               | 66.3257  | 96.9532              |
| 3.38643  | 1.8912               | 10.3902  | 10.9026              | 72.1684  | 107.496              |
| 3.6846   | 2.2638               | 10.6428  | 10.5602              | 78.493   | 118.287              |
| 4.00939  | 2.67478              | 10.8956  | 10.3329              | 85.4014  | 129.288              |
| 4.36405  | 3.12648              | 11.0778  | 10.2123              | 92.9166  | 141.948              |
| 4.74998  | 3.60269              | 11.1482  | 10.1722              | 101.078  | 155.308              |
| 5.1699   | 4.11007              | 11.2561  | 10.1554              | 109.992  | 168.972              |
| 5.627    | 4.68991              | 12.2502  | 9.66278              | 119.68   | 184.9                |
| 6.13012  | 5.32562              | 13.3283  | 9.48185              | 130.228  | 201.719              |
| 6.67389  | 6.03284              | 14.5022  | 9.59019              | 141.718  | 219.511              |
| 7.10413  | 6.63156              | 15.7814  | 10.114               | 154.278  | 240.96               |
| 7.25699  | 6.85195              | 17.1714  | 11.0322              | 167.83   | 260.642              |
| 7.35752  | 7.02592              | 18.6841  | 12.3673              | 182.682  | 277.423              |
| 7.61062  | 7.42826              | 20.329   | 14.0904              | 198.75   | 290.055              |
| 7.86347  | 7.87388              | 22.119   | 16.4224              | 216.218  | 304.325              |
| 7.89874  | 7.92861              | 24.0674  | 19.2722              | 235.233  | 318.568              |
| 8.11664  | 8.36093              | 26.1899  | 22.6617              | 255.879  | 334.717              |
| 8.36967  | 8.90483              | 28.4972  | 26.1836              | 278.172  | 357.458              |
| 8.59826  | 9.44914              | 31.0118  | 30.5314              | 301.822  | 395.891              |
| 8.62288  | 9.53177              | 33.7455  | 35.5319              |          |                      |
| 8.87629  | 10.2817              | 36.7235  | 41.0953              |          |                      |
| 9.12994  | 11.2571              | 39.9639  | 47.4717              |          |                      |